

# Multiphoton Emission

G. Díaz Camacho,<sup>1</sup> E. Zubizarreta Casalengua,<sup>2</sup> J. C. López Carreño,<sup>3</sup>  
S. Khalid,<sup>2</sup> C. Tejedor,<sup>1</sup> E. del Valle,<sup>1,4,2</sup> and F. P. Laussy<sup>2,5</sup>

<sup>1</sup>*Departamento de Física Teórica de la Materia Condensada & IFIMAC,  
Universidad Autónoma de Madrid, 28049 Madrid, Spain*

<sup>2</sup>*Faculty of Science and Engineering, University of Wolverhampton, Wulfruna St, Wolverhampton WV1 1LY, UK*

<sup>3</sup>*Institute of Theoretical Physics, University of Warsaw, ul. Pasteura 5, 02-093, Warsaw, Poland*

<sup>4</sup>*Institute for Advanced Study, Technical University of Munich,  
Lichtenbergstrasse 2a, D-85748 Garching, Germany.*

<sup>5</sup>*Russian Quantum Center, Novaya 100, 143025 Skolkovo, Moscow Region, Russia\**

(Dated: September 27, 2021)

We describe the emission, detection and structure of multiphoton states of light. We include the effect of frequency filtering, which describes, at a fundamental level, physical detection of a quantum emitter. The case of the spontaneous emission of Fock states is treated fully and analytically. We stress this picture by contrasting it to the numerical simulation of two-photon bundles emitted from a two-level system in a cavity. We show that dynamical factors exist that allow for a more robust multiphoton emission than spontaneous emission. We also describe how this relates to thermal light.

Multiphoton (or multiquanta) physics is rapidly emerging in various areas of quantum technology [1–8]. Nonetheless, a detailed description of basic and fundamental aspects of its emission and detection is still lacking. In this Letter, we provide the foundations for a general description of multiphoton dynamics. Namely, we give exact closed-form expressions for the full photon-counting probabilities of the frequency-filtered Spontaneous Emission (SE) of Fock states, from which we derive their complete temporal structure and thus all statistical observables of possible interest. We discuss particular cases for illustration and then contrast SE to Continuous Wave (CW) emission as well as thermal equilibrium.

To give the most general description, we compute directly the probability  $p(n, T; t)$  of detecting  $n$ -photons in the time window between  $t$  and  $t+T$ . For a single-mode source with bosonic annihilation operator  $a$  and emission rate  $\gamma_a$ , this is given by Mandel's formula [9, 10]  $p(n, T; t) = \frac{1}{n!} \langle : \Omega^n \exp(-\Omega) : \rangle$  with  $:$  denoting normal ordering and  $\Omega$  the time-integrated intensity operator  $\Omega(t, T) \equiv \xi \gamma_a \int_t^{t+T} (a^\dagger a)(t') dt'$ ,  $\xi$  quantifying detection efficiency (1 for a perfect detector). This quantity is more general than the more popular Glauber correlation functions  $g^{(n)}$  [11], that can be derived from it either in their theoretical form or as measured in experiments. Their connection is apparent through  $G^{(m)}(t_1, \dots, t_m) \equiv \theta(t_1 < t_2 < \dots < t_m) \langle a^\dagger(t_1) \dots a^\dagger(t_m) a(t_m) \dots a(t_1) \rangle +$  (all other time ordering), with  $\theta$  the Heavyside function. Substituted in Mandel's formula, this yields:

$$p(n, T; t) = \frac{(-1)^n}{n!} \sum_{k=0}^{\infty} \frac{(-\xi \gamma)^{n+k} (n+k)!}{k!} \int_t^{t+T} \dots \int_t^{t_3} \int_t^{t_2} \langle a^\dagger(t_1) \dots a^\dagger(t_{n+k}) a(t_{n+k}) \dots a(t_1) \rangle dt_1 dt_2 \dots dt_{n+k}. \quad (1)$$

We now turn to the computation of Eq. (1) in cases of interest for multiphoton physics. The simplest and

most fundamental type of multiphoton emission is that of a group, or “bundle” [12–15], of  $N$  photons, emitted spontaneously by a source, e.g., a passive cavity of natural frequency  $\omega_a$  in the state  $\rho(0) = |N\rangle\langle N|$  at  $t = 0$ , that freely radiates its photons at the rate  $\gamma_a$  without any type of stimulation or other dynamical factor. Under these conditions, the state evolves according to the Lindblad master equation (we set  $\hbar = 1$ )  $\dot{\rho} = -i\omega_a [a^\dagger a, \rho] + \frac{\gamma_a}{2} (2a\rho a^\dagger - a^\dagger a\rho - \rho a^\dagger a)$  which can be easily integrated to yield the  $m$ th order diagonal correlators as  $\langle a^\dagger m a^m \rangle(t) = \frac{N!}{(N-m)!} e^{-m\gamma_a t}$ . To compute Eq. (1), we need the multi-time correlators  $\langle :(\prod_{k=1}^n a(t_k))^\dagger \prod_{k=1}^n a(t_k): \rangle$ , that can be found with the quantum regression formula, e.g., for  $m = 1$ , one has  $\langle a^\dagger(t'_1) a(t_1) \rangle = \langle a^\dagger a \rangle(0) e^{-(\gamma_a/2-i\omega_a)t'_1} e^{-(\gamma_a/2+i\omega_a)t_1}$  regardless of the time order. For SE, this can, through a tedious but systematic procedure, be generalized thanks to the same structure being maintained to higher orders, namely,  $\langle a^\dagger(t'_1) \dots a^\dagger(t'_m) a(t_m) \dots (t_1) \rangle = \frac{N!}{(N-m)!} (\prod_{\kappa=1}^m e^{-(\gamma_a/2-i\omega_a)t'_\kappa}) (\prod_{k=1}^m e^{-(\gamma_a/2+i\omega_a)t_k})$  from which one can subsequently compute the quantum-average for any power of  $\Omega$  by splitting its time-dynamics from the operator  $a^\dagger a$  in a scalar function  $\mathcal{T}$  as  $\Omega(t, T) = \mathcal{T}(T) a^\dagger(t) a(t)$ . For SE, with  $\Omega(0, T) = \gamma_a \xi \left( \int_0^T e^{-\gamma_a t} dt \right) a^\dagger(0) a(0)$ , we have:

$$\mathcal{T}(T) = \xi (1 - e^{-\gamma_a T}). \quad (2)$$

With time and quantum-averages now separated, it is straightforward to compute  $\langle : \Omega^k : \rangle = \mathcal{T}^k \langle a^\dagger k a^k \rangle(0) = \xi^k (1 - e^{-\gamma_a T})^k \frac{N!}{(N-k)!}$  for all  $1 \leq k \leq N$  which, when substituted in Mandel's formula (now keeping track in the notation of the initial state  $N$  instead of the initial time  $t$ ),  $p(n, T; N) = \sum_{k=n}^{\infty} (-1)^{n+k} \langle : \Omega^k : \rangle / (n!(k-n)!)$ , simplifies to the physically transparent form:

$$p(n, T; N) = \binom{N}{n} \mathcal{T}(T)^n (1 - \mathcal{T}(T))^{N-n} \quad (3)$$

that is, a binomial distribution arising from independent Bernoulli trials for the detection of a single photon in the time  $T$ . Variations of this result have been known for a long time [16, 17] and, with hindsight, Eqs. (2) and (3) could have been postulated based on physical arguments. Equation (2) is indeed the probability to detect a single photon in SE in the time window  $[0, T]$  and thus corresponds to the quantum efficiency.

The value of the above derivation is, besides a rigorous and direct justification of the result, its extension to the case of filtered emission. At a fundamental level, frequency filtering describes detection [18, 19] since any physical detector has a finite temporal resolution and consequently a frequency bandwidth, which restricts the quantum attributes of the measured system. Ultimately, any quantum system has to be observed and at this point, instead of being a mere technical final step, detection typically brings all the counter-intuitive and disruptive nature of the theory. Including these fundamental constraints is therefore essential for a physical theory of multiphoton emission. To do that, the previous derivation can be repeated but now involving filtered-field operators  $\varsigma(t) \equiv \int_{-\infty}^{\infty} \mathcal{F}(t - t_1) a(t_1) dt_1$  whereby a filter  $\mathcal{F}$  is applied to the source's field. For SE, the time dynamics can similarly be separated from the quantum operator  $\varsigma(t) = \Xi(t) a(0)$  that now combines both the dynamics of filtering and SE in  $\Xi \equiv \int_{-\infty}^{+\infty} \mathcal{F}(t - t_1) e^{-(\frac{\gamma_a}{2} + i\omega_a)t_1} \theta(t_1) dt_1$ . In this way, the filtered time-integrated intensity operator from  $[0, T]$ , which is needed for Mandel's formula, reads  $\Omega_{\Gamma}(T) = \gamma_a \xi \int_0^T \varsigma^\dagger \varsigma(t) dt = \mathcal{T}_{\Gamma}(T) (a^\dagger a)(0)$ . This provides the single-photon-detection probability for a filtered-field  $\mathcal{T}_{\Gamma}(T) = \gamma_a \xi \int_0^T \Xi_{\mathcal{F}}(t)^* \Xi_{\mathcal{F}}(t) dt$ . In the case of interference (Lorentzian) filters  $\mathcal{F}(t) = \frac{\Gamma}{2} e^{-(\Gamma/2 + i\omega_a)t} \theta(t)$  and SE,  $\Xi(t) = (\Gamma/\Gamma_-) (e^{-(\gamma_a/2 + i\omega_a)t} - e^{-(\Gamma/2 + i\omega_1)t}) \theta(t)$ , in which case, defining  $\Gamma_{\pm} \equiv \Gamma \pm \gamma_a$ , the quantum efficiency to use in Eq. (3) for a physical detector, or to describe the filtering of light, is:

$$\mathcal{T}_{\Gamma}(T) = \frac{\Gamma}{\Gamma_+} - \frac{\Gamma^2 e^{-\gamma_a T} + \Gamma \gamma_a e^{-\Gamma T}}{\Gamma_-^2} + \frac{4\Gamma^2 \gamma_a e^{-\Gamma + T/2}}{\Gamma_-^2 \Gamma_+}. \quad (4)$$

It generalizes Eq. (2), which it recovers in the limit  $\Gamma \rightarrow \infty$  since, due to Heisenberg uncertainty, one must detect at all the frequencies and loose this information, to know precisely when the photons are being detected. Also, the quantum efficiency is now tending to  $\Gamma/\Gamma_+$  for infinite integration times  $T$ , i.e., the probability to detect a filtered SE photon, or with some knowledge of its frequency, is less than 1, even for a perfect detector ( $\xi = 1$ ), due to its finite bandwidth, showing again the fundamental interplay of time and frequency in the detection. From this result, we can now describe completely the SE of  $N$  photons with or without filtering. This comes in the form of the joint probability distribu-

tion function (pdf)  $\phi^{(N)}(\{t_k\})$  for the  $k$ th photon to be detected at time  $t_k$ . We derive this quantity from its link to the photon counting probability Eq. (1) by defining  $p(t_1, \dots, t_N)$  the probability to detect the  $k$ th photon *up to* time  $t_k$  as  $p(\{t_k\}) = \int_0^{\tau_1} \dots \int_0^{\tau_N} \phi^{(N)}(\{\tau_k\}) \prod_{i=1}^N d\tau_i$ . Since the latter is related to the single-photon detection probabilities as  $N! \mathcal{T}(t_1) \prod_{k=1}^{N-1} (\mathcal{T}(t_{k+1}) - \mathcal{T}(t_k))$  [20], one can obtain  $\phi(t_1, \dots, t_N) = \frac{\partial^N}{\partial t_1 \dots \partial t_N} p(t_1, \dots, t_N)$  from the fundamental theorem of calculus. We give directly the filtered emission result, from which unfiltered emission arises as the limiting case  $\Gamma \rightarrow \infty$  (it is explicated in [20]):

$$\phi_{\Gamma}^{(N)}(t_1, \dots, t_N) = N! \gamma_a^N \times \left( \frac{\Gamma}{\Gamma_-} \right)^{2N} \prod_{i=1}^N (e^{-\Gamma t_i/2} - e^{-\gamma_a t_i/2})^2 \mathbb{1}_{[t_{i-1}, t_{i+1}]}(t_i) \quad (5)$$

where  $\mathbb{1}_T(t)$  is the indicator function which is 1 if  $t \in T$  and 0 otherwise. This time-domain restriction temporally correlates the photons (the  $k$ th photon can only be emitted after all the previous  $k-1$  photons have been), while their dynamics is otherwise the same as can be seen from the symmetry of the expression (5). This provides the exact and complete temporal structure of multiphoton SE, and is one of the main results of this work (the  $N = 2$  case is shown in Fig. 1(a)). From it, one can compute all the statistical quantities regarding filtered multiphoton SE. As an illustration, we derive the marginal distributions for the emission of each photon in isolation  $\phi_{\Gamma, k}^{(N)}(t_k) \equiv \int \dots \int \phi(t_1, \dots, t_N) \prod_{j \neq k} dt_j$  and, from there, emission time averages  $\langle t_k^{(N)} \rangle \equiv \int_0^{\infty} t_k \phi_{\Gamma, k}^{(N)}(t_k) dt_k$  (we consider variances, etc., in the supplementary material [20]). The one-photon marginals are less fundamental and general than the full joint pdf (5), but they are more familiar, accessible and practical. We find  $\phi_{\Gamma, k}^{(N)}(t_k) \equiv - \left( \frac{\Gamma}{\Gamma_-} \right)^{2N} \gamma_a^N k \binom{N}{k} g(t_k)^{N-k} (g(t_0) - g(t_k))^{k-1} g'(t_k)$  where we defined  $g(t) \equiv \frac{e^{-\gamma_a t}}{\gamma_a} + \frac{e^{-\Gamma t}}{\Gamma} - 4 \frac{e^{-\Gamma + t/2}}{\Gamma_+}$  so that  $g'(t) = -(e^{-\Gamma t/2} - e^{-\gamma_a t/2})^2$ —the term that enters in Eq. (5)—makes the integration of the marginal tractable in the form of nested integrals [20]  $\int_{t_0}^{t_k} \dots \int_{t_{k-2}}^{t_k} \int_{t_k}^{\infty} \dots \int_{t_{N-1}}^{\infty} \prod_{i=1}^N g'(t_i) dt_1 \dots dt_{k-1} dt_{k+1} \dots dt_N$ . The distributions  $\phi_{\Gamma, k}^{(N)}(t_k)$  are for the  $k$ th photon from a fully-detected  $N$ -photon bundle. To take into account that filtering removes some photons, one needs to turn to the conditional probabilities  $\varphi_k^{(N)}(t)$  of detecting the  $k$ th photon regardless of how many photons have been detected. This is obtained as the probability to detect the photon in the  $k$ th position in a  $N$ -photon bundle of which  $n$  photons have been detected, the probability of which is Eq. (3), so that, from the law of total probability [20],  $\varphi_n^{(N)}(t_n) \equiv \sum_{k=n}^N \frac{P(k, N)}{P(k, k)} \phi_{\Gamma, n}^{(k)}(t_n)$ , with  $\varphi_n^{(N)}$  directly normalized to the fraction of  $n$ -photon-bundles

detected in the SE of  $N$  photons:

$$\mathcal{N}(n, N) \equiv \sum_{k=n}^N P(k, N) = \frac{\Gamma_+^n}{\Gamma_+^N} \binom{N}{n} {}_2F_1(1, n-N, n+1, -\Gamma) \quad (6)$$

where  ${}_2F_1$  is the Hypergeometric function. In particular,  $\mathcal{N}(n, N)$  is the probability to detect  $n$  photons from a  $N$ -photon bundle, with  $\mathcal{N}(N, N) = (\Gamma/\Gamma_+)^N$  the fraction of fully-detected bundles (no photon lost), in agreement with the filtered quantum efficiency derived previously. Qualitatively, the detected photons are delayed and spread, with earlier photons being more impacted. A representative case is shown in Fig. 1(b), for the case  $N = 5$  and filter widths  $\Gamma/\gamma_a = 1, 5$  and  $25$ , the latter case of which starts to be qualitatively close to the case of unfiltered emission. This is for  $\varphi$ , i.e., corresponding to unconditioned detections. The case conditioned to full-bundle detection is shown in the upper part for  $\Gamma/\gamma_a = 1$  where one can see how incomplete bundles result in further spreading out the photons and piling them up towards the later times. Note that the 5th photon distribution is the same in both cases since these are detected only when the bundle remains unbroken. From all the possible statistical observables (a long list is given in the Supplementary Material [20] along with their derivations), it should be enough here to contemplate the mean time of detection for the  $k$ th photon of a  $N$ -photon bundle, which, although it could seem a simple quantity, actually requires an 11-indices summation of multinomials to combine decay-rate and filtering:

$$\langle t_k^{(N)} \rangle = k\gamma_a^N \left( \frac{\Gamma_+}{\Gamma} \right)^N \left( \frac{\Gamma}{\Gamma_-} \right)^{2N} \binom{N}{k} \sum_{\{k_i\}} \binom{N-k}{k_1, k_2, k_3} \times \frac{(-1)^{k_3+k_6+k_7+k_8+k_{11}} \binom{2}{k_{10}, k_{11}} \binom{k-1}{k_4, k_5, k_6, k_7, k_8, k_9}}{\gamma_a^{\Sigma_1} \Gamma^{\Sigma_2} \left( \frac{\Gamma_+}{4} \right)^{\Sigma_3} (\Sigma_4 \gamma_a + \Sigma_5 \Gamma + \frac{\Gamma_+}{2} (k_3 + k_9))^2} \quad (7)$$

where  $\sum_{\{k_i\}} \equiv \sum_{k_1+k_2+k_3=N-k} \sum_{k_4+\dots+k_9=k-1} \sum_{k_{10}+k_{11}=2}$  and  $\Sigma_1 \equiv k_1 + k_4 + k_7$ ,  $\Sigma_2 \equiv k_2 + k_5 + k_8$ ,  $\Sigma_3 \equiv k_3 + k_6 + k_9$ ,  $\Sigma_4 \equiv k_1 + k_7 + \frac{k_{11}}{2}$ ,  $\Sigma_5 \equiv k_2 + k_8 + \frac{k_{10}}{2}$  the various combinations involved.

This generalizes the unfiltered photons result  $\lim_{\Gamma \rightarrow \infty} \langle t_k^{(N)} \rangle = (H_N - H_{N-k})/\gamma_a$  (with  $H_N$  the  $N$ th harmonic number and assuming  $H_0 \equiv 0$ ), explaining the observed photon-bundle time length (measured as the time between the first and last detected photons)  $\langle \tau \rangle_N \equiv \langle t_N^{(N)} \rangle - \langle t_1^{(N)} \rangle$  that goes to  $H_{N-1}/\gamma_a$  in this limit, as was observed in Refs. [12, 15], as well as the  $k$ th photon lifetime measured as  $\langle t_k^{(N)} \rangle - \langle t_{k-1}^{(N)} \rangle \rightarrow 1/(\gamma_a k)$  as was observed in Refs. [21, 22]. In the opposite limit, the same harmonic structure is found but this time governed by the filter alone with no direct influence (to leading order) from the radiative decay, with  $\langle t_k^{(N)} \rangle \sim (H_N - H_{N-k})/\Gamma$  as  $\Gamma \rightarrow 0$  so that we have the

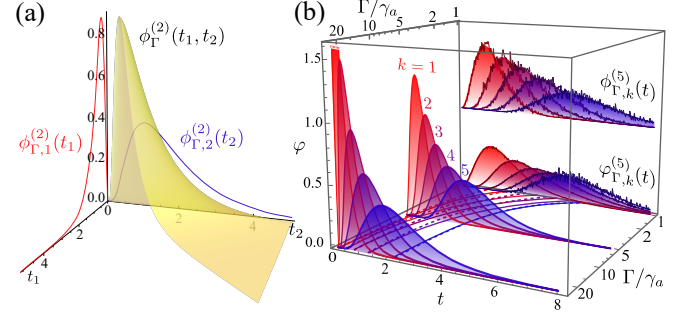


FIG. 1. Filtered  $N$ -photon spontaneous emission. (a) For  $N = 2$  photons, one can visualize the full pdf  $\phi_{\Gamma}^{(2)}(t_1, t_2) = 2\gamma_a^2(\Gamma/\Gamma_-)^4 g'(t_1)g'(t_2)\mathbf{1}_{[t_1, \infty]}(t_2)$  in addition to its marginals  $\phi_{\Gamma,k}^{(2)}(t_k)$  which are its projections on the single-photon subspaces. (b) Marginals for  $N = 5$  for various filter widths  $\Gamma$ , conditioned ( $\phi$ , up) or not ( $\varphi$ , down) to full-bundle detection. The case  $\Gamma/\gamma_a = 1$  has superimposed a numerical simulation. On the floor, the mean times (7) showing dilation of the bundles under filtering (solid for  $\varphi$ , dashed for  $\phi$ ).

important limits:

$$\langle \tau \rangle_N = \frac{H_{N-1}}{\Gamma} \text{ at small } \Gamma \text{ and } \frac{H_{N-1}}{\gamma_a} \text{ at large } \Gamma. \quad (8)$$

To unify these two simple and symmetric cases, one has to use Eq. (7), which illustrates how awkward the transition from one limit to another can be even for such a basic problem of mere SE. The time-dilation of the filtered bundle is shown on the floor of Fig. 1(b). We also consider a richer, more accessible and more insightful statistical quantity that will further allow us to generalize our discussion to other types of multiphoton emission, namely, the waiting-time distribution (wtd), i.e., the probability distribution for the time difference between successive photons. For the SE of a two-photon bundle, this is obtained from Eq. (5) as  $w_2(\tau) = \int_0^\infty \phi_{\Gamma}^{(2)}(t, \tau+t) dt$  which gives:

$$w_2(\tau) = \frac{\Gamma \gamma_a (\Gamma + \gamma)}{(\Gamma - \gamma_a)^2 (3\Gamma + \gamma) (\Gamma + 3\gamma_a)} (\Gamma (3\Gamma + \gamma_a) e^{-\gamma_a \tau} + \gamma_a (\Gamma + 3\gamma_a) e^{-\Gamma \tau} - 8\Gamma \gamma_a e^{-\frac{\Gamma + \gamma_a}{2} \tau}). \quad (9)$$

This is a tri-exponential decay that balances the radiative decay with its filtering. This quantity provides another way to the average time length of a two-photon bundle as a function of filtering  $\langle \tau \rangle_2 = \int_0^\infty \tau w_2(\tau) d\tau = \frac{1}{\Gamma} + \frac{1}{\gamma_a} + \frac{2}{\gamma_a + \Gamma} - \frac{9}{4(3\Gamma + \gamma_a)} - \frac{9}{4(\Gamma + 3\gamma_a)}$  (this is, alternatively, obtained from Eq. (7) as  $\langle t_2^{(2)} \rangle - \langle t_1^{(2)} \rangle$ ), which recovers the limits (8) with numerator  $H_2 = 1$ .

This completes our description of filtered SE of Fock states, which is the starting point and reference for all other types of multiphoton emission, for instance, the steady-state  $N$ -photon emission of Ref. [12]. We focus on the simplest case  $N = 2$  but similar conclusions apply

to all  $N$ . We simulate numerically with a frequency-resolved Monte Carlo method [23] a filtered “bundler” (emitter of bundles), whose principle and implementation is detailed in Ref. [12]. This is the result of a coherently driven Jaynes-Cummings Hamiltonian in the dispersive limit, that can also be understood as a Purcell-enhanced Mollow-triplet and is thus clearly a rich system. We compare both its wtd and its photon-purity  $\pi_2$  (the percentage of unbroken bundles or photons emitted in pairs) with a toy-model of CWSE (continuous wave spontaneous emission) that simulates the actual emission of the bundler with randomly triggered SE of two-photon Fock states. For the most part, we find that the multiphoton emission from the bundler behaves accordingly to the SE of collapsed Fock states, as has been suggested all along [24]. Their wtd, shown in Fig. (a) for different purities (50% and 100%), share the same qualitative main features. The multiphoton peak, in particular, i.e., the short-time excess of probabilities due to photons piling up from the multiphotons, behaves similarly under filtering. This is shown in Fig. (b) where numerically simulated CWSE and two-photon bundlings are superimposed on the theoretical  $\langle\tau\rangle_2$  given after Eq. (9). There are, nevertheless, noteworthy quantitative departures, most prominently, the greater robustness of the bundles to filtering, as seen in Fig. (c) where the purity corresponds to that of SE with an effective decay rate of  $\approx\gamma_a/2$ , so that for the same filter width, bundles originating from the driven system (bundler) are significantly more likely to be fully detected than if they were emitted by SE. This is surprising given the otherwise excellent agreement with a picture of collapsed Fock states that are subsequently spontaneously emitted. One can track this departure to the dynamics of the emitter itself (the two-level system) that, upon collapsing, resets the SE process in a mechanism akin to the quantum Zeno effect [25] that effectively slows down the emission, i.e., reduces  $\gamma_a$ . This, in turn, makes the multiphoton detection more robust, as explained again by filtered SE which is indeed better for larger  $\Gamma/\gamma_a$ . This dynamical enhancement depends on various parameters such as the statistics of the bundles themselves, which warrants a study on its own. This suggests, however, that the prospects of improving multiphoton emission by frequency filtering are even better than has been anticipated [26].

Finally, one cannot address multiphoton emission without considering the most famous and pervading case, which has been foundational to quantum optics [27] and whose role remains central for applications [28], let alone this being the most common type of light, namely, the thermal state. This is obtained by supplementing the Lindblad master equation of SE with a pumping term  $\frac{P_a}{2}(2a^\dagger pa - aa^\dagger \rho - \rho aa^\dagger)$  where  $P_a < \gamma_a$  drives the cavity to a steady state  $\rho = (1 - \theta) \sum_{n=0}^{\infty} \theta^n |n\rangle \langle n|$  with effective temperature  $\theta \equiv P_a/\gamma_a$ . We can now precise its perceived relationship to multiphoton emission by compar-

ing thermal light to the cases above of pure multiphoton emission. The Laplace transform of the wtd is obtained from the same transform of the  $g^{(2)}(\tau)$  function [29] as  $\tilde{w}_2(s) = (1 + 1/[\gamma_a n_a \tilde{g}^{(2)}(s)])^{-1}$  which gives

$$w_{\text{th}}(\tau) = \frac{2P_a \gamma_a}{(\gamma_a - P_a) Q_a} \left\{ Q_a \cosh \left[ \frac{Q_a \tau}{2(\gamma_a - P_a)} \right] - 2P_a \gamma_a \sinh \left[ \frac{Q_a \tau}{2(\gamma_a - P_a)} \right] \right\} \exp \left[ -\frac{\gamma_a^2 + P_a^2}{2(\gamma_a - P_a)} \tau \right] \quad (10)$$

where we have defined  $Q_a^2 \equiv P_a^4 - 4P_a^3 \gamma_a + 10P_a^2 \gamma_a^2 - 4P_a \gamma_a^3 + \gamma_a^4$ . This has a similar shape (cf. Fig. (a, green dotted line)) than the wtd of all the types of multiphoton emission previously described, but behaves distinctively under filtering. To take only the average time of the multiphoton peak: in the limit of large-bandwidth filtering, one recovers the unfiltered case and thus, from Eq. (10), one can obtain the asymptote as the average of the multiphoton peak of a thermal state, which is  $\langle\tau_\infty\rangle_{\text{th}} = (\gamma_a - P_a)/(P_a^2 + \gamma_a^2 + Q_a)$  and is shown in the inset of Fig. (b): in units of  $\gamma_a$ , it is a quantity between 0 (when  $P_a \rightarrow \gamma_a$  with the multiphoton peak becoming a Dirac  $\delta$  function) and 1 (when  $P_a \rightarrow 0$  with the multiphoton peak reducing to two-photon bunching and thus to the radiative lifetime). A first qualitative difference with pure multiphoton emission is therefore that this quantity is continuous, instead of quantized (through the Harmonic numbers). The other difference is found when looking at the evolution of thermal multiphoton peak average  $\langle\tau_\Gamma\rangle_{\text{th}}$ , with narrowing filtering  $\Gamma$ . A first surprise is that although filtering has a tendency to thermalize quantum states, and does this exactly in the limit  $\Gamma \rightarrow 0$  for all physical states, filtering a thermal state does *not* produce another thermal state, despite the fact that all the Glaubler correlators of the filtered thermal field  $g_\Gamma^{(n)}(0) = n!$  remain the same. Their time dynamics, however, exhibit a different trend [20]. Since in the limit  $\Gamma \rightarrow 0$ , a thermal state is nevertheless recovered as a universal limit, one can still obtain the asymptotic behaviour, which is the same inverse filter width dependence, that goes like  $\langle\tau_0\rangle_{\text{th}} \gamma_a = \langle\tau_\infty\rangle_{\text{th}} (1 - \theta)/\Gamma$ . This disconnection of the two limits, as compared to Eq. (8), makes it again qualitatively differing from pure multiphoton emission, even if it is filtered and thus starts to feature bundles of various sizes. Indeed, in this case, one finds that the multiphoton peak in the wtd yields  $\langle\tilde{\tau}\rangle_N \equiv \sum_{k=2}^N \frac{\langle t_k \rangle - \langle t_1 \rangle}{k-1} P(k, N) / \sum_{k=2}^N P(k, N)$ . Note that except for  $N = 2$ , the bundle time length  $\langle\tilde{\tau}\rangle_N$  does not coincide with the multiphoton peak average  $\langle\tilde{\tau}\rangle_N$  in the two-photon wtd. The latter is obtained by weighting the contribution of each sub-bundle population, meaning that filtered  $N$ -photon bundles breaks down into an essentially  $(N-1)$ -type of bundle, then  $N-2$ , etc. down to 2 photon emission with the surviving bundles thus converging to the asymptote of this case. The thermal

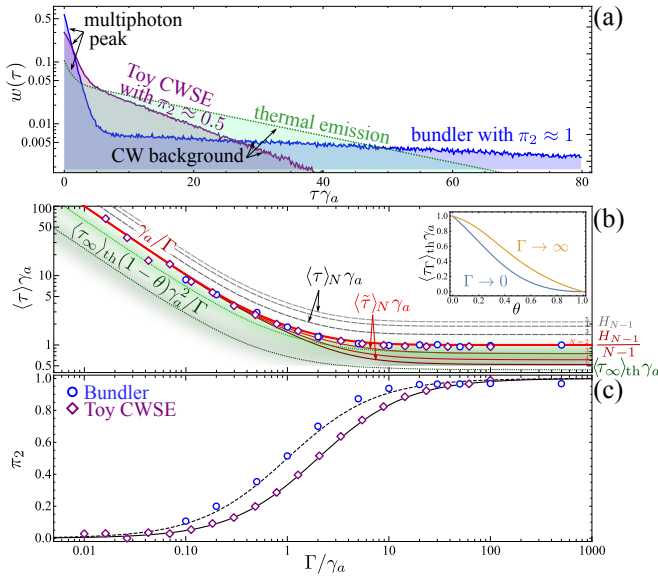


FIG. 2. Dynamical multiphoton emission. (a) wtd for the toy-model (CWSE of Fock states, purple), the bundler (blue) and a thermal state (dotted green), all featuring a multiphoton peak sitting on the background separating multiphotons. The toy model and bundler would be identical if they had the same purity. (b) Multiphoton peak average as a function of filtering, for the case of pure multiphoton emission  $\langle \tilde{\tau} \rangle_N$  for  $N$  from 2 to 5, exhibiting quantization at large  $\Gamma$  and a unique asymptote at small  $\Gamma$  when all bundles are broken into two-photon ones. The toy-model (purple diamonds) and the bundler (blue circles) behave according to the SE picture (red thick line). In contrast, the filtered thermal multiphoton-peak averages  $\langle \tau \rangle_{th}$  are not quantized (shading) and retain multiphoton contributions to all orders. In inset, average of the thermal multiphoton peak in its wtd as a function of  $\theta \equiv P_a/\gamma_a$  leading to different asymptotes. Dashed gray lines:  $N$ -photon bundle time lenght  $\langle \tau \rangle_N$  also featuring same coefficients for the asymptotes. (c) Two-photon purity [percentage of fully detected bundles] from Fock state SE (line), the toy-model (diamonds) and the bundler (circles) which higher purity fits well with a SE rate of  $\approx \gamma_a/2$  (dotted lines).

case, in stark contrast, maintains thermal contributions from multiphotons of all sizes, regardless of the filtering. Therefore, even if their wide-filter asymptotes match, their narrow-filter trends depart as shown in Fig. (b), with, therefore, also dynamical features present in thermal equilibrium that break from the paradigm of SE. This provides, we believe, a first insightful relationship and departure between a thermal state and pure multiphoton sources. Their closest encounter is at vanishing temperature where a thermal state then behaves as a two-photon emitter but with almost all its bundles broken... a fairly subtle and elusive connection!

In conclusion, we have provided a comprehensive and analytical description of the fundamental case of SE of Fock states, illustrated with statistical observables of interest. Compared to other types of multiphoton emission,

we have shown that although a bundler behaves in all respect as SE of collapsed Fock states, dynamical features exist that protect bundles, making them significantly more resilient to filtering than if they were generated by SE. This calls for further studies to understand, characterize and exploit such dynamical advantages. We have also highlighted connections and departure with thermal light, which features multiphoton emission to all orders of a different character than pure multiphoton emission with broken bundles to all orders. Such characterizations could also be made for superchaotic light, superbunching, leapfrog processes in resonance fluorescence, etc., which should enlighten on the nature, character and relationship of these sources with pure multiphoton emission, thus allowing to establish a zoology of its various types.

FPL acknowledges support from Rosatom, responsible for the roadmap on quantum computing. EdV acknowledges the CAM Pricit Plan (Ayudas de Excelencia del Profesorado Universitario) and the TUM-IAS Hans Fischer Fellowship and projects AEI / 10.13039/501100011033 (2DEnLight). CT acknowledges the Agencia Estatal de Investigación of Spain, under contract PID2020-113445GB-I00 and, with EdV, the Sinérgico CAM 2020 Y2020/TCS-6545 (NanoQuCoCM).

\* [fabric.e.lauss@gmail.com](mailto:fabric.e.lauss@gmail.com)

- [1] Hofheinz, M. *et al.* Synthesizing arbitrary quantum states in a superconducting resonator. *Nature* **459**, 546 (2009). URL [doi:10.1038/nature08005](https://doi.org/10.1038/nature08005).
- [2] Sayrin, C. *et al.* Real-time quantum feedback prepares and stabilizes photon number states. *Nature* **477**, 73 (2011). URL [doi:10.1038/nature10376](https://doi.org/10.1038/nature10376).
- [3] Chu, Y. *et al.* Creation and control of multi-phonon fock states in a bulk acoustic-wave resonator. *Nature* **563**, 666 (2018). URL [doi:10.1038/s41586-018-0717-7](https://doi.org/10.1038/s41586-018-0717-7).
- [4] Deléglise, S. *et al.* Reconstruction of non-classical cavity field states with snapshots of their decoherence. *Nature* **455**, 510 (2008). URL [doi:10.1038/nature07288](https://doi.org/10.1038/nature07288).
- [5] Sánchez Muñoz, C. & Schlawin, F. Photon correlation spectroscopy as a witness for quantum coherence. *Phys. Rev. Lett.* **124**, 203601 (2020). URL [doi:10.1103/PhysRevLett.124.203601](https://doi.org/10.1103/PhysRevLett.124.203601).
- [6] nas Boström, E. V., D’Andrea, A., Cini, M. & Verdonzzi, C. Time-resolved multiphoton effects in the fluorescence spectra of two-level systems at rest and in motion. *Phys. Rev. A* **102**, 103719 (2020). URL [doi:10.1103/PhysRevA.102.013719](https://doi.org/10.1103/PhysRevA.102.013719).
- [7] Zhong, H.-S. *et al.* Quantum computational advantage using photons. *Science* **370**, 1460 (2020). URL [doi:10.1126/science.abe8770](https://doi.org/10.1126/science.abe8770).
- [8] Uria, M., Solano, P. & Hermann-Avigliano, C. Deterministic generation of large fock states. *Phys. Rev. Lett.* **125**, 093603 (2020). URL [doi:10.1103/PhysRevLett.125.093603](https://doi.org/10.1103/PhysRevLett.125.093603).
- [9] Mandel, L. Fluctuations of photon beams: The distribution of the photo-electrons. *Proc. Roy. Soc* **74**, 233

(1959). URL [doi:10.1088/0370-1328/74/3/301](https://doi.org/10.1088/0370-1328/74/3/301).

[10] Kelley, P. L. & Kleiner, W. H. Theory of electromagnetic field measurement and photoelectron counting. *Phys. Rev.* **136**, A316 (1964). URL [doi:10.1103/PhysRev.136.A316](https://doi.org/10.1103/PhysRev.136.A316).

[11] Glauber, R. J. Photon correlations. *Phys. Rev. Lett.* **10**, 84 (1963). URL [doi:10.1103/PhysRevLett.10.84](https://doi.org/10.1103/PhysRevLett.10.84).

[12] Sánchez Muñoz, C. *et al.* Emitters of  $N$ -photon bundles. *Nature Photon.* **8**, 550 (2014). URL [doi:10.1038/nphoton.2014.114](https://doi.org/10.1038/nphoton.2014.114).

[13] Bin, Q., Lü, X.-Y., Laussy, F. P., Nori, F. & Wu, Y.  $n$ -phonon bundle emission via the stokes process. *Phys. Rev. Lett.* **124**, 053601 (2020). URL [doi:10.1103/PhysRevLett.124.053601](https://doi.org/10.1103/PhysRevLett.124.053601).

[14] Bin, Q., Wu, Y. W. & Lü, X.-Y. Parity-symmetry-protected multiphoton bundle emission. *Phys. Rev. Lett.* **127**, 073602 (2021). URL [doi:10.1103/PhysRevLett.127.073602](https://doi.org/10.1103/PhysRevLett.127.073602).

[15] Cosacchi, M. *et al.* Suitability of solid-state platforms as sources of  $n$ -photon bundles. *arXiv:2108.03967* (2021).

[16] Scully, M. O. & W. E. Lamb, J. Quantum theory of an optical maser. III. Theory of photoelectron counting statistics. *Phys. Rev.* **179**, 368 (1969). URL [doi:10.1103/PhysRev.179.368](https://doi.org/10.1103/PhysRev.179.368).

[17] Arnoldus, H. F. & Nienhuis, G. Photon correlations between the lines in the spectrum of resonance fluorescence. *J. Phys. B.: At. Mol. Phys.* **17**, 963 (1984). URL [doi:10.1088/0022-3700/17/6/011](https://doi.org/10.1088/0022-3700/17/6/011).

[18] Eberly, J. & Wódkiewicz, K. The time-dependent physical spectrum of light. *J. Opt. Soc. Am.* **67**, 1252 (1977). URL [doi:10.1364/JOSA.67.001252](https://doi.org/10.1364/JOSA.67.001252). TDS1.3.

[19] del Valle, E., González-Tudela, A., Laussy, F. P., Tejedor, C. & Hartmann, M. J. Theory of frequency-filtered and time-resolved  $n$ -photon correlations. *Phys. Rev. Lett.* **109**, 183601 (2012). URL [doi:10.1103/PhysRevLett.109.183601](https://doi.org/10.1103/PhysRevLett.109.183601).

[20] Díaz Camacho, G. *et al.* Supplementary material. (*online*) (2021).

[21] Wang, H. *et al.* Measurement of the decay of fock states in a superconducting quantum circuit. *Phys. Rev. Lett.* **101**, 240401 (2008). URL [doi:10.1103/PhysRevLett.101.240401](https://doi.org/10.1103/PhysRevLett.101.240401).

[22] Brune, M. *et al.* Process tomography of field damping and measurement of Fock state lifetimes by quantum nondemolition photon counting in a cavity. *Phys. Rev. Lett.* **101**, 240402 (2008). URL [doi:10.1103/PhysRevLett.101.240402](https://doi.org/10.1103/PhysRevLett.101.240402).

[23] López Carreño, J. C., del Valle, E. & Laussy, F. P. Frequency-resolved Monte Carlo. *Sci. Rep.* **8**, 6975 (2018). URL [doi:10.1038/s41598-018-24975-y](https://doi.org/10.1038/s41598-018-24975-y).

[24] Strekalov, D. V. Cavity quantum electrodynamics: A bundle of photons, please. *Nature Photon.* **8**, 500 (2014). URL [doi:10.1038/nphoton.2014.144](https://doi.org/10.1038/nphoton.2014.144).

[25] Misra, B. & Sudarshan, E. C. G. The Zeno's paradox in quantum theory. *J. Math. Phys.* **18**, 756 (1977). URL [doi:10.1063/1.523304](https://doi.org/10.1063/1.523304).

[26] Sánchez Muñoz, C., Laussy, F. P., del Valle, E., Tejedor, C. & González-Tudela, A. Filtering multiphoton emission from state-of-the-art cavity QED. *Optica* **5**, 14 (2018). URL [doi:10.1364/OPTICA.5.000014](https://doi.org/10.1364/OPTICA.5.000014).

[27] Hanbury Brown, R. & Twiss, R. Q. Correlation between photons in two coherent beams of light. *Nature* **177**, 27 (1956). URL [doi:10.1038/177027a0](https://doi.org/10.1038/177027a0).

[28] Valencia, A., Scarcelli, G., D'Angelo, M. & Shih, Y. Two-photon imaging with thermal light. *Phys. Rev. Lett.* **94**, 063601 (2005). URL [doi:10.1103/PhysRevLett.94.063601](https://doi.org/10.1103/PhysRevLett.94.063601).

[29] Kim, M., Knight, P. & Wodkiewicz, K. Correlations between successively emitted photons in resonance fluorescence. *Opt. Commun.* **62**, 385 (1987). URL [doi:10.1016/0030-4018\(87\)90005-8](https://doi.org/10.1016/0030-4018(87)90005-8).